The role of deposition temperature and scanning speed in the functional performance of laser assisted cold sprayed (LACS) coatings.

E. O. Olakanmi[1*]; O. P. Oladijo[2]; B. A. Obadele[3]

[1]Department of Mechanical, Energy & Industrial Engineering; Botswana International University of Science & Technology, Palapye, Botswana.

[2]Department of Chemical, Metallurgical & Materials Engineering; Botswana International University of Science & Technology, Palapye, Botswana.

[3]Department of Chemical Engineering; University of Johannesburg, Doornfontein Campus, Johannesburg, South Africa.

Abstract:

The functional performance of laser assisted cold sprayed (LACS) commercially pure (CP) grade 1 titanium coatings was elucidated in terms of its mechanism of densification, microstructural evolution and corrosion resistance as the deposition temperature and scanning speed were altered by employing optical microscopy (OM) and potentio-dynamic polarization technique. The outcome of this study indicates that the densification mechanism of the coating was mainly influenced by the ratio of the processing temperature (T) and the scanning speed (SS) which is designated as $T/_{SS}$. The attainment of the optimised functional properties of the coatings could be attributed to the thermal shear in the titanium film as well as its solid state inter-particulate consolidation resulting from localised thermal gradient which was induced between the ductile titanium particles and the brittle oxide film covering it at the optimum laser-gas-material interaction obtained at 600ºC/10mm/s coupled with the adiabatic shearing of the particles upon impact at the deposition site. It was also established that microstructural porosity and cracks resulted from the increased lifetime of the liquid phase under sub-optimal processing conditions which allowed more time for the propellant gas to initiate bubble formation within the coating's microstructure. In addition, non-optimal parameters failed to attain the most desirable microstructural properties and corrosion resistance for the coatings. Finally, key factors in optimising LACS process parameters in order to achieve fully dense coatings are outlined.

*Corresponding author. Tel.: +26774276012

E-mail address: olakanmie@biust.ac.bw

1. Introduction

Engineering materials such as austenitic stainless steels (Type 304L) encounter extreme severe wear and thermal plastic strains arising from environmental degradation occasioned by high chamber pressure and heat fluxes operating conditions. This eventually weakens the materials structurally such that they are deficient in load-bearing capacity at elevated temperature. In addition, engineering materials' functional performance such as wear, oxidation and corrosion resistance also diminish under high temperature operating conditions. These operational challenges necessitate that damaged engineering parts are deposited with coating materials in an attempt to extend the operational life and increase the reliability of the components. Grade 1 commercially pure (CP) titanium (Ti) is a typical coating material that could be used for this purpose. It is an un-alloyed grade designed for excellent weldability, good strength, impact toughness, ductility and corrosion resistance (Obadele *et al.,* 2015).

Laser assisted cold spray (LACS) is a hybrid manufacturing process which employs heat from laser beam to soften cold sprayed (CS) powdered particles for deposition on the substrate (Olakanmi & Doyoyo, 2014; Olakanmi, 2015). LACS deposits a wider range of materials including hard metals by using cheaper nitrogen gas relative to CS process which only deposits soft materials via expensive inert gases (Bray *et al.,* 2009; Lupoi *et al.,* 2011). LACS is also preferable to CS because it deposits materials at a temperature much below its melting point and reduced critical deposition velocity which results in fabricating fully-dense and thicker coatings in a single spray pass (Bray *et al.,* 2009; Lupoi *et al.,* 2011). Moreover, coatings manufactured with LACS do not suffer from processing problems such as oxidation, part distortion and formation of undesirable intermetallic phases which result in poor mechanical properties in comparison to traditional coating manufacturing processes such as vacuum plasma spray, laser cladding and high velocity oxy-flame processes (HVOF) (Bray *et al.,* 2009; Lupoi *et al.,* 2011; Olakanmi *et al.,* 2013). Three variants of LACS described by Olakanmi & Doyoyo (2014) included pre-treatment in which the laser beam passes millisecond prior to the cold spray jet; concentric coupling of the cold spray process with laser beam for softening the substrates and powdered particles; and post-cold spray laser treatment.

Bray *et al.,* (2009) and Lupoi *et al.,* (2011) successfully applied LACS to deposit oxide free, fully dense titanium coatings; characterised by an average hardness of 272 $HV_{0.3}$ and a bond strength in excess of 77 MPa; by employing processing temperatures between 650 to 900 ºC, well below the melting point of titanium (1668 °C). Olakanmi *et al.,* (2013) elucidated the deposition mechanism of LACS as softening of metal powder particles via laser irradiation and adiabatic shearing at optimum processing parameters. The corrosion behaviour of cold sprayed CP Ti coatings in natural sea water and 3.5 wt% NaCl solution was assessed by Hussain and co-investigators (2011) and Marrocco *et al.,* 2011) and Wang *et al.,* (2007). The outcome of these studies indicated that porosity degraded the corrosion response of these coatings in comparison bulk titanium sample (Hussain *et al.,* 2011a). Meanwhile, it was demonstrated that laser glazing of the cold sprayed CP titanium coatings eliminated surface porosity within its microstructure as indicated by improved corrosion resistance which was similar to that of the bulk titanium. However, analysis of these cited literature reveals that no study has been undertaken to examine the relationship between LACS processing parameters, the mechanism of consolidation, microstructural properties and corrosion resistance of LACS deposited CP Ti (grade 1) coatings in different

media. In order to extend the frontiers of knowledge of LACS deposited coatings, this study was undertaken to explore the effects of LACS processing temperature and scanning speed on the mechanism of densification, microstructural properties and corrosion performance of CP Ti (grade 1) coatings in 3.0 % NaCl and 1 M HCl environment.

2. Materials & Methodology

Gas atomised CP Ti (grade 1) powders (TLS Technik GmbH, +45 to -90 µm particle size and distribution) having spherical morphology was used to determine the effects of LACS processing temperature and scanning speed on the mechanism of consolidation, microstructural properties and corrosion performance of titanium coatings. In agreement with Bray *et al.,* (2009), Lupoi *et al.,* (2011) and Olakanmi *et al.,* (2013, 2015); the adopted powder size and distribution used in this study was selected because it is less expensive relative to the narrow-band CS powders. The coating was deposited on 304L stainless steel with dimensions 100 mm x 50 mm x 5 mm. Prior to depositing the coating on the substrate, the surfaces of the substrates were roughened by grit blasting with a view to ensuring strong adhesion of the coating to the 304L stainless steel substrate.

A 4.4 kW Nd-YAG (ROFIN DY 044) laser system of 1.06 mm wavelength and a AT-1200HPHV 500PSI (35 bar) powder feeder resident at the Council for Scientific and Industrial Research/National Laser Centre (CSIR/NLC), Pretoria, South Africa were used to deposit the coatings. The DLV-180 nozzle (converging–diverging type) developed at the Institute for Manufacturing (ifM), Cambridge, United Kingdom and used to spray the titanium particles was mounted on Kuka robot such that the operator controlled the equipment within a safety enclosure. The nozzle is characterised by a round exit of 6mm diameter, expansion ratio of 9, divergent section length of 180 mm, throat diameter of 2 mm, and total length of 210 mm. The Nd:YAG laser system was operated with a 600 micron step index fiber delivered to a beam shaping module having a 200 mm focal length (FL) collimator and a Precitec YW50 unit fitted with a FL lens. It produced a beam having an approximate spot size of 5.0 mm and a top hat intensity distribution.

A high pressure nitrogen (N_2) gas was employed in propelling the particles of CP Ti (Grade 1) from the AT-1200HPHV 500PSI (35 bar) powder feeder into the nozzle. The nitrogen gas was split and sent directly to the nozzle; and via the powder feeder. At the nozzle, the titanium particles mixed with the nitrogen gas. Thereafter, both titanium particles and N_2 gas stream were re-combined and propelled through the nozzle at supersonic speed for deposition at the substrate. The powder-laden jet and the laser irradiation impacted concentrically on a region of the substrate. LACS deposition temperature was measured real-time and varied via a LASCON® high-speed infrared pyrometer (temperature range 400–1000 ºC) having a response time of 10 µs and accuracy of ±0.5% of the measured value. The data from the pyrometer were fed through a closed-loop feedback control system which altered laser power with a view to maintaining the desired temperature. The use of pyrometer to control the laser power was meant to soften both the titanium particles and the substrate at a sub-melting temperature so as to deform and build up coatings at sub-sonic impact velocity (Bray *et al.,* 2009;

Lupoi *et al.,* 2011). The spraying nozzle was held perpendicular to the substrate's surface with the laser beam positioned at an angle of 15º to the surface normal.

Varied parameters used in this study included scanning speed (5, 7.5 and 10 mm/s) and processing temperature (600 and 750 ºC) with the gas pressure, powder feed rate, and stand-off distance set at constant values of 30 bar, 25.0 rpm and 34.7 mm respectively. The constant experimental parameters were chosen in line with the laboratory standards developed at the CSIR/NLC, Pretoria. Meanwhile, future investigations will explore the effects of combining different LACS parameters by using design of experiments (DoE) technique. The specified range of scanning speed and deposition temperature was to ensure appropriate laser-cold-gas-material interaction which prevents non-bonding of titanium particles to the substrate or to one another or the formation of molten pool which leads to the development of intermetallics and distortion of the substrate (Bray *et al.,* 2009; Olakanmi, 2015). Multiple tracks of coatings were made for each deposition temperature at varied scanning speeds at 50% overlap.

The procedure described in Olakanmi *et al.,* (2013; 2015) was adopted in preparing cross-section of coating samples; taking from the middle of the tracks where the deposition was continuous; for microstructural characterisation. Density of the coatings was determined according to the procedure described in Goyal *et al.,* (2013). Microstructural observation of the coatings was undertaken via optical microscope (OM) (Olympus BX51M). The analySIS FIVE image analysis software was used to calculate the area fraction of pores within the optical micrograph of polished cross-sections of samples in an attempt to estimate the amount of porosity in the coatings. The Vickers microhardness values of the coatings was measured using a Future-tech Vickers microhardness tester at a load of 100 gf (1.0 N) and dwell time of 10s.. Polished titanium coatings were etched in Kroll's reagent with a view to observing the nature of grain boundary/phase transformation in the coatings. Electrochemical corrosion tests were performed in of 3.5% NaCl and 1 M HCl solutions at room temperature. Specimens were prepared by attaching an insulated copper wire using aluminium tape to one face of the specimen and cold mounted in an epoxy resin. The specimens were ground to surface finish with 1200-grit SiC papers. Thereafter, the specimens were ultrasonically cleaned in ethanol before immersion in the solutions for corrosion test. Electrochemical tests were carried out using an Autolab potentiostat (PGSTAT30 computer controlled). The corrosion potential, E_{corr} and corrosion current density, I_{corr} were calculated by analyses of the Tafel region using the General Purpose Electrochemical Software (GPES) version 4.9. All the experiments were conducted in a three electrode cell with saturated Ag/AgCl (3 M KCl) as reference electrode, graphite rod as counter electrode and the specimens as the working electrode. Potentiodynamic polarization test was implemented using a scan rate of 2 mV.s^{-1} at a potential initiated at -0.7 V to 0.3 V. The tests started after 60 min of free exposure to the electrolyte in order to obtain stable open circuit potential.

3. Results and Discussion

3.1. Effects of variation in processing temperature and scanning speed on the densification mechanism of LACS deposited titanium coatings.

Fig. 1 shows the variation of the density of the LACS deposited titanium coatings with processing temperature and scanning speed. Each measurement of density is an average of three readings. It is evident from Figure 1 that the density of the coatings increases directly with the scanning speed while it decreases with the processing temperature. Meanwhile, Fig. 2 which shows the porosity analysis of coatings as determined by analySIS FIVE image analysis software lends credence to the findings from Fig. 1.
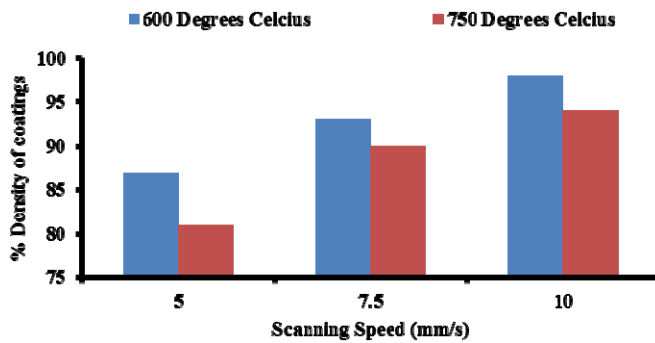

Fig. 1: Effects of processing temperature and scanning speed on the density of titanium coatings.

Meanwhile, the density of the coating can also be influenced by the ratio of the processing temperature (T) and the scanning speed (SS) which is designated as $T/_{SS}$. Fig. 3 depicts an indirect relationship between the density of titanium coatings and the $T/_{SS}$ ratio. Reduced coating density reported at higher $T/_{SS}$ ratio could be accounted for by titanium deposits attaining a semi-molten state which upon solidification produces deleterious effects of porosity within the microstructure. By comparing LACS to other laser material processing (LMP) techniques such as selective laser sintering/melting (SLS/SLM); pore formation in the coatings could be explained by the increased lifetime of the semi-liquid phase of titanium deposits which allowed more time for pore formation upon the propellant nitrogen gas forming bubbles in the coatings during processing (Olakanmi *et al.,* (2011, 2013). However, increased density of coatings noted at lower $T/_{SS}$ ratio could be attributed to the titanium deposit which did not reach the semi-molten state, hence, it was able to solidify at a faster rate before the formation of nitrogen bubbles within the deposits.
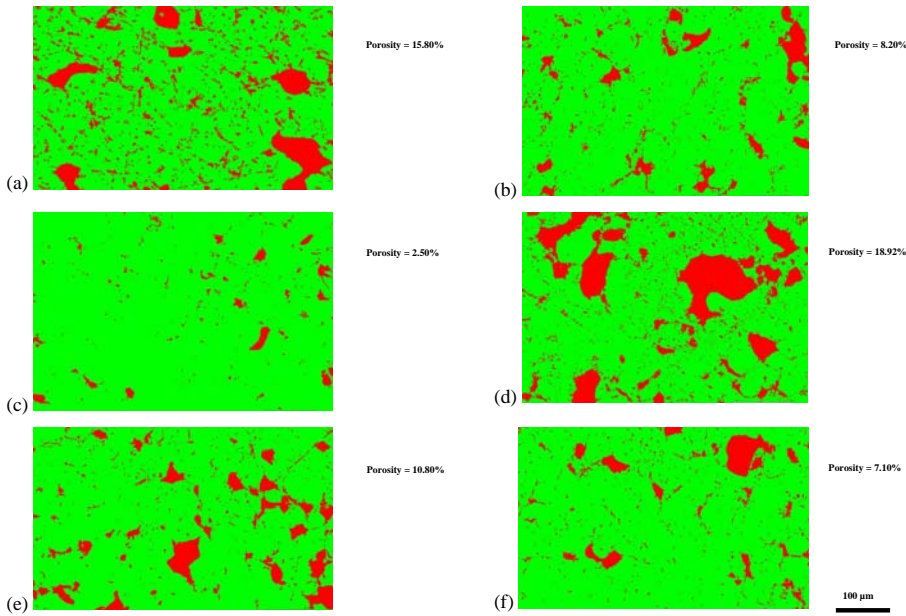
Fig. 2: Porosity analysis in the LACS-deposited titanium coatings produced with various LACS processing parameters: (a) 600 ºC and 5 mm/s (b) 600 ºC and 7.5 mm/s (c) 600 ºC and 10.0 mm/s (d) 750 ºC and 5 mm/s (e) 750 ºC and 7.5 mm/s (f) 750 ºC and 10.0 mm/s

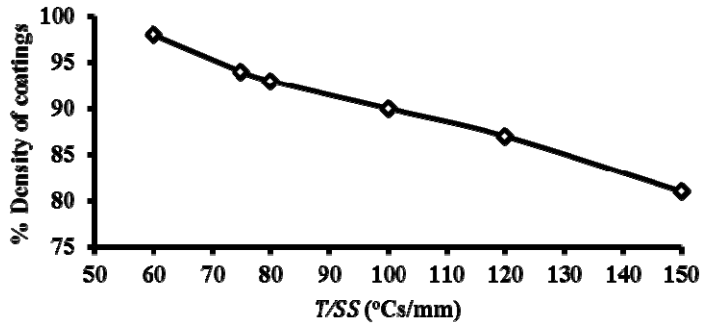Fig. 3: Effects of T/SS ratio on the density of titanium coatings.

3.2. Effects of processing temperature and scanning speed on the microstructural evolution of LACS deposited titanium coatings.

Polished microstructures which reveal the pore structure of titanium coatings deposited via LACS under varying processing conditions are shown in Fig. 4. Analysis of the micrographs indicates that the connectivity and orientation of the pores in the coatings are function of LACS processing condition. For example, nearly dense coatings were produced by adopting 600 ºC and 10 mm/s as processing parameters which corresponds to the lowest $T/_{SS}$. ratio (Fig. 4c) with its microstructure characterised with isolated and irregular pores having average sizes of approximately 50 µm. At higher $T/_{SS}$ ratio as shown in Fig. 4a, b, d, e and f, the microstructure of the coatings are noted to be less dense due to occurrence of interconnected and irregular micro-porosity characterised with sizes of approximately 250 µm. Density values (81 to 94%) reported for coatings deposited with $T/_{SS}$ ratios varying between 80 to 150 ºCs/mm in Figure 3 attest to this claim. Similar to the microstructure of cold sprayed coatings, it is seen that all the LACS deposited titanium coatings are also characterised by surface porosities. This could be attributed to the absence of tamping action induced by follow-up spray process (Marrocco *et al.,* 2006; Wong *et al.,* 2011).
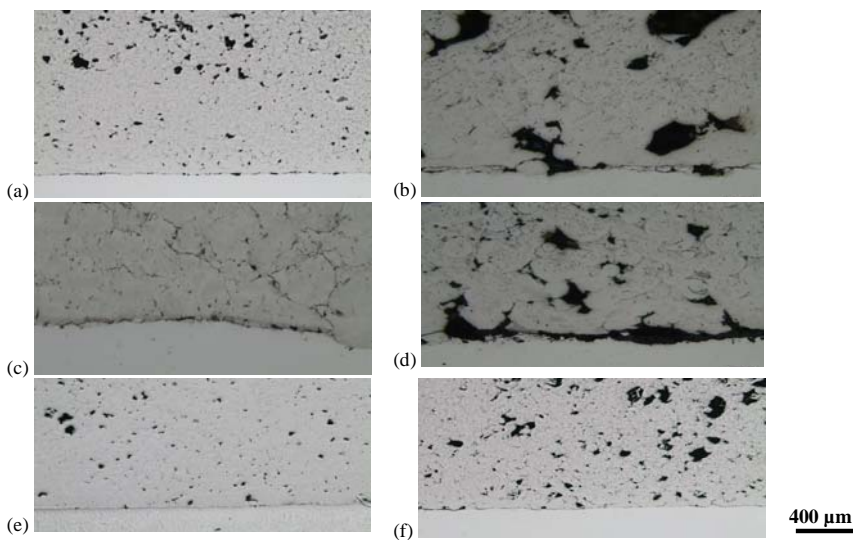

Fig. 4: Optical micrographs of LACS deposited titanium coatings under varying processing conditions (a) 600 ºC and 5 mm/s (b) 600 ºC and 7.5 mm/s (c) 600 ºC and 10.0 mm/s (d) 750 ºC and 5 mm/s (e) 750 ºC and 7.5 mm/s (f) 750 ºC and 10.0 mm/s

The formation of a strong and coherent bonding between the coating and the substrate in Fig. 4c is evident by non-existence of porosity or crack at the interface. By comparing the microstructural interface in Figure 4c to that of Fig. 4a, b, d, e and f, it is clear that the microstructural interface of coatings produced with higher $T/_{SS}$ ratios is characterised by porosity and cracks. This indicates lesser degree of occurrence of mechanical anchorage of the particles to the substrate in coatings produced with higher $T/_{SS}$ ratios relative to that of Fig. 4c. Furthermore, the processing temperatures as measured by the pyrometer in this study were less than the melting point of titanium (1,638 °C).

The existence of porosities and cracks in the coatings upon microstructural solidification at higher $T/_{SS}$ ratios points to the formation of semi-molten state of titanium deposits during processing. Even though this is not expected, however, the occurrence of semi-molten state during LACS processing indicates that the temperature regime developed within the coating deposits at higher $T/_{SS}$ ratios is nearly or even above the melting temperature of titanium. This may be accounted for by the temperature rise due to the synergetic effects of adiabatic shearing on one hand as well as the processing temperature/scanning speed interactions on the other hand. A check through Fig. 4 shows the non-existence of unbonded titanium particles within the microstructure unlike the occurrence during LACS processing of aluminium and aluminium alloys (Olakanmi *et al.,* 2013; 2015). Non-existence of unbonded particles in titanium coatings deposited at higher $T/_{SS}$ ratios supports the possibility that the pure titanium particles used in this study are uniformly thick and have oxide film thickness greater than or equal to a thresholding value below which oxide film cracking will not occur. In addition, Ma *et al.,* (2015) reported noticeable dissolution of the surface oxide film on titanium powder starts from the temperature range of 615–674 °C during heating depending on powder characteristics. Meanwhile, the attainment of the optimised microstructural properties of the coatings could be attributed to the thermal shear in the film as well as its solid state inter-particulate consolidation resulting from localised thermal gradient which was induced between the ductile titanium particles and the brittle film covering it at the optimum laser-gas-material interaction obtained at 600 °C/10mm/s coupled with the adiabatic shearing of the particles upon impact at the deposition site.

Fig. 5. Microhardness profiles of LACS-deposited titanium coatings deposited at varying $T/_{SS}$ ratios

Fig. 5 presents the microhardness profile for LACS deposited coatings at varying $T/_{SS}$ ratios. It is evident that uniform values of microhardness obtained for the coating produced with $T/_{SS}$ ratio (60 °Cs/mm) confirms the homogeneity of its microstructure in the absence of porosity or crack (Fig. 5). Non-uniformity in the microhardness profiles of the coatings produced with $T/_{SS}$ ratios other than 60 °Cs/mm supports our findings that porosity and cracks did occur in their microstructures.
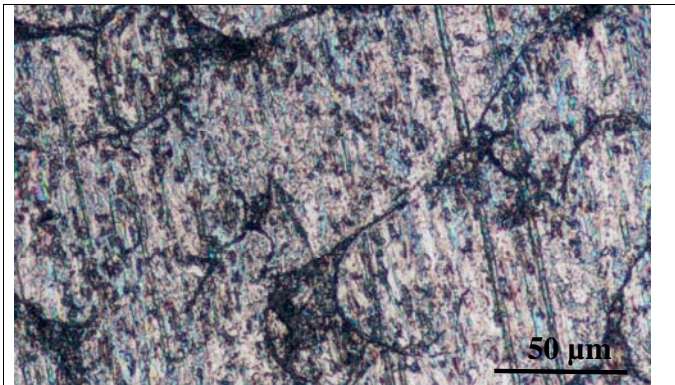
Fig. 6. Etched microstructure of LACS deposited titanium coating fabricated with 600 ºC and 10.0 mm/s showing occurrence of recrystalisation process which resulted in the formation of fine grains upon the elimination of particle boundaries

Analysis of the microstructure of the coatings fabricated with 600 ºC and 10.0 mm/s revealed the occurrence of recrystalisation process which resulted in the formation of fine grains upon the elimination of particle boundaries (Fig. 6). This phenomenon could be elucidated by the application of appropriate LACS processing parameters which induced an annealing effect on the sprayed particles due to suitable cooling rate which allowed for grain recovery (Zahiri *et al.*, 2009). Therefore, the elimination of particle boundaries and formation of grain boundaries points to occurrence of improved metallurgical bonding in the coatings at the specified LACS parameters.

3.3. Effects of variation in processing conditions on the corrosion behaviour of LACS deposited titanium coatings.

Fig. 7 represents the potentio-dynamic polarization plot which was employed to determine corrosion behaviour such as corrosion potential and corrosion current for LACS deposited coatings in different media. For 3.5 wt% NaCl solution, it can be inferred from Fig. 7a that the substrate displayed the least corrosion potential of about -0.54 V when compared to all LACS samples. Sample deposited at 600 ºC-5 mm/s showed the noblest corrosion potential at -0.35 V while samples cladded at 750 ºC- 7.5, 10 mm/s recorded the least potentials (-0.50 and -0.49 V). Generally, it is clear from Figure 7a that all the LACS deposited samples demonstrated significant improvement in corrosion potential in 3.5 wt% NaCl solution as seen from the displacement of cathodic and anodic curves. However, for all the LACS samples, there is a shift in the anodic corrosion current density towards a higher current density, indicating lower corrosion resistance compared to the substrate. Nevertheless, all LACS samples demonstrated higher pitting potential when compared to the substrate. The pitting potential for the substrate is -0.21 V while that for sample cladded at 600 ºC-10 mm/s is far above 0.2 V. This is an indication that the current plateau of 600 ºC-10 mm, is significantly stable –with no passivation-repassivation stages (breakdown potentials) observed on the anodic branch of the polarisation curves. This behaviour could be associated with the degree of porosity measured on the surface of 600 ºC-10 mm/s. From Figure 2, it could be seen that sample cladded at 600 ºC-10 mm/s showed the least porosity and this invariably contributed to the stable current plateau observed. In other words, samples with more pores on the surface tend to have more

==active sites for corrosion initiation.== Generally, none of both cladded and 304 steel samples displayed an active region in the polarization plots after the Tafel region but they entered directly into a stable passive region.

The potentiodynamic polarisation curves for all LACS samples and substrate in 1 M HCl is shown in Fig. 7b. It could be seen that the range of values for the open circuit potential for all the samples is relatively small (-0.34 V). ==In addition, all of the samples showed an active-passive region in the polarization plots following the Tafel region but they entered directly into active region as compared to their response in 3.5% NaCl solution.== When the anodic corrosion current densities were determined via linear extrapolation of the Tafel polarization plots, Table 1 reveals that there is no significant difference in the anodic current densities as compared to the substrate. This indicates that the corrosion behaviour of the substrate (i.e. 304 ASS) could be compared to that of the titanium substrate. The formation of stable TiO_2 layer could improve the corrosion-resistant of LACS coatings and as such could be compared to austenitic stainless steel. Yaya *et al.,* (2015) had reported that the corrosion behaviour of CP Ti is more resistant than 316 austenitic stainless steel. Hence, it can be inferred that LACS processing conditions strongly influence the corrosion performance of the coatings.
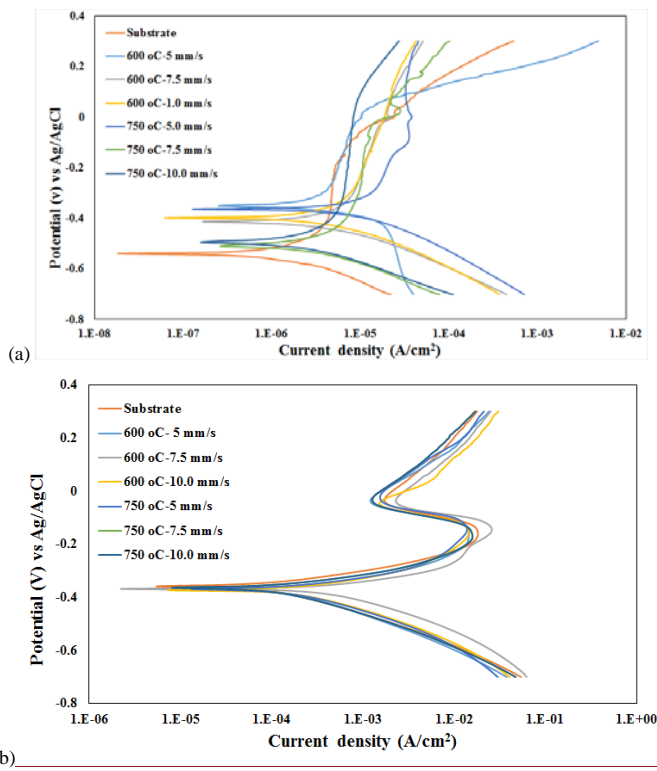

(a)

(b)

Fig. 7. Comparative analysis of potentio-dynamic polarization curves for LACS deposited coatings in (a) 3 wt% NaCl and (b) 1 M HCl solution.

From Table 1, for 1 M HCl solution, all the samples displayed similar corrosion potential as well as anodic current densities values. Furthermore, the anodic current densities in 1 M HCl solution is significantly higher than in 3.5% NaCl. This shows that these coatings would display high corrosion rate in 1 M HCl solution

Table 1: Corrosion parameters as a function of LACS parameters

Sample	Corrosion potential (E_{corr}) (V)		Anodic current density (I_{corr}) (A/cm^2)	
	3.5% NaCl	1 M HCl	3.5% NaCl	1 M HCl
Substrate	-0.54	-0.37	4.83μ	0.008
600 ºC - 5 mm/s	-0.35	-0.36	6.30μ	0.008
600 ºC – 7.5 mm/s	-0.41	-0.37	12.20μ	0.007
600 ºC – 10.0 mm/s	-0.40	-0.37	13.50μ	0.010
750 ºC – 5.0 mm/s	-0.36	-0.35	17.80μ	0.009
750 ºC – 7.5 mm/s	-0.51	-0.36	10.90μ	0.006
750 ºC – 10.0 mm/s	-0.50	-0.36	7.05μ	0.006

4.0 Conclusions

The target of this study was to examine the densification mechanism as well as the microstructural and corrosion characterisation of CP Ti (grade 1) coatings via optical microscopy (OM) and open cell circuits and potentio-dynamic tests as LACS processing temperature and scanning speed were varied. The outcome of this study indicates that the densification mechanism of the coating was mainly influenced by the ratio of the processing temperature (T) and the scanning speed (SS) which is designated as $T/_{SS}$. Densification mechanism, microstructural properties and corrosion resistance in 3.5 wt% NaCl solution were optimised at the lowest $T/_{SS}$ ratio. This is consequent upon the thermal shear in the film covering titanium particles as well as its solid state inter-particulate consolidation resulting from localised thermal gradient which was induced between the ductile titanium particles and the brittle film covering it at the optimum laser-gas-material interaction obtained at 600ºC/10mm/s coupled with the adiabatic shearing of the particles upon impact at the deposition site. The use of LACS deposited CP titanium (grade 1) coatings in 3.5 wt% NaCl media is recommended while its use in the HCl environment is not suitable at present. Further study need to be carried out to determine appropriate additive to be incorporated into the coating to improve its corrosion in an acidic medium. Finally, it is important that a DoE technique is employed to explore the influence of combining the LACS process parameters on the quality characteristics of titanium coatings.

References:

Bray, M.; Cockburn, A.; O'Neill, W., 2009. The laser-assisted cold spray process and deposit characterisation. Surface Coating Technology 203 (19), 2851–2857.

Goyal, T.; Walia, R. S.; Sidhu, T. S. 2013. Multi-response optimisation of low-pressure cold-sprayed coatings through Taguchi method and utility concept. International Journal of Advanced Manufacturing Technology 64 (5–8), 903–914.

Hussain, T., McCartney, D., Shipway, P., Marrocco, T., 2011. Corrosion behavior of cold sprayed titanium coatings and free standing deposits, Journal of Thermal Spray Technology 20 (1), 260–274.

Lupoi, R.; Sparkes, M.; Cockburn, A.; O'Neill, W., 2011. High speed titanium coatings by supersonic laser deposition. Material Letters 65 (21–22), 3205–3207.

Ma, Q., Ya, Y., Luo, F., Shudong, D., Tang, H. P., 2015. Pressureless sintering of titanium and titanium alloys: sintering densification and solute homogenization, in "*Titanium powder metallurgy: science, technology and applications*". In: Ma, Q., Francis, H. F. (Eds.), Elsevier, Kidlington, Oxford, pp. 201. (doi:10.1016/B978-0-12-800054-0.00012-5)

Marrocco, T., McCartney, D. G., Shiway, P. H., Sturgeon, A. J., 2006. Production of titanium deposits by cold-gas dynamic spray: numerical modeling and experimental characterization, Journal of Thermal Spray Technology 15 (2), 263–272.

Marrocco, T., Hussain, T., McCartney, D., Shipway, P., 2011. Corrosion performance of laser posttreated cold sprayed titanium coatings, Journal of Thermal Spray Technology 20(4), 909–917.

Obadele, B. A., Olubambi., P. A., Andrews, A., Pityana, S., Mathew, M. T., 2015. Electrochemical behaviour of laser-clad Ti_6Al_4V with CP Ti in 0.1 M oxalic acid solution. Journal of Alloys and Compounds 646, 753-759.

Olakanmi, E. O.; Cochrane, R. F.; Dalgarno, K. W. 2011. Densification mechanism and microstructural evolution in selective laser sintering of Al-12Si powders. Journal of Materials Processing Technology, 211 (1), 113–121.

Olakanmi, E.O.; Tlotleng, M.; Meacock, C.; Pityana, S.; Doyoyo, M., 2013. Deposition mechanism and microstructure of Laser Assisted Cold Sprayed (LACS) Al-12wt%Si coatings: Effects of laser power. Journal of the Minerals, Metals & Materials Society (TMS) (Journal of Materials: JOM) 65 (6), 776–783.

Olakanmi, E. O.; Doyoyo, M., 2014. Laser assisted cold sprayed coatings: A review. Journal of Thermal Spray Technology 23 (5), 765–785.

Olakanmi, E. O., 2015. Optimization of the Quality Characteristics of Laser-Assisted Cold-Sprayed (LACS) Aluminium Coatings with Taguchi Design of Experiments (DOE), Materials and Manufacturing Processes (DOI: 10.1080/10426914.2014.984306)

Wang, H.-R., Li, W-Y., Ma, L., Wang, J., Wang, Q., 2007. Corrosion behaviour of cold sprayed titanium protective coating on 1Cr13 substrate in seawater, Surface & Coating Technology 201 (9–11), 5203–5206.

Wong, W., Irissou, E., Ryabinin, A., Legoux, J. –G., Yue, S., 2011. Influence of helium and nitrogen gases on the properties of cold gas dynamic sprayed pure titanium coatings, Journal of Thermal Spray Technology 20 (1), 213–226.

Yaya, K., Khelfaoui, Y., Malki, B., Kerkar, M. 2011. Numerical simulations study of the localized corrosion resistance of AISI 316L

stainless steel and pure titanium in a simulated body fluid environment. Corrosion Science 53, 3309-3314.

Zahiri, S. H., Fraser, D., Jahedi, M., 2009. Recrystallization of cold spray-fabricated CP titanium structures, Journal of Thermal Spray Technology 18 (1), 16–22.